

# SYNTHESIS AND CHARACTERIZATION, MORPHOLOGY, THERMAL STABILITY, AND MAGNETIC PROPERTIES OF $\alpha$ -Fe<sub>2</sub>O<sub>3</sub> USING LIQUID-LIQUID INTERFACE REACTION

Jyothilaxmi<sup>1</sup>, and H.V. Vijayanand<sup>2\*</sup>, Dhondiba. V<sup>3</sup> A. Venkataraman<sup>4</sup>

<sup>1</sup> PDA College of Engineering, Kalaburagi

<sup>2</sup> Government College (Autonomous), Kalaburagi

<sup>3</sup> Government First Grade College Women's Kalaburgi

<sup>4</sup> Department of Chemistry Gulbarga University, Kalaburgi

**Abstract:** The solid-state reaction begins at the surface of the reactant. It is well-known fact that, decrease in particle size up to the nano scale, increases the surface area and hence, the number of adsorption sites. It is reported that porous alumina when prepared employing different synthetic routes, show excellent behavior. One of the possible explanations given is that the octahedral aluminum sites are fully occupied while vacant sites are randomly disturbed at the tetrahedral positions. These vacant sites in the structure are mainly responsible for the adsorption behavior on  $\alpha$ -Al<sub>2</sub>O<sub>3</sub> surface. In contrast to  $\alpha$ -Al<sub>2</sub>O<sub>3</sub>, which adopt normal spinel structure,  $\alpha$ -Fe<sub>2</sub>O<sub>3</sub> possess inverse spinel structure with vacancies in the octahedral sites. The present study describes about the synthesis of  $\alpha$ -Fe<sub>2</sub>O<sub>3</sub> and CuO, metal oxides using liquid-liquid interface reaction.

**Key words:** Liquid-liquid interface, metal oxides, and characterization

## 1. Introduction

### • Nanomaterials

Different periods in the history of human civilization are named after the materials used e.g. Stone Age, Bronze Age, Iron Age, Polymer age, etc. Presently, it is the age of Nanomaterials. These materials are mostly inorganic or organic compounds having interesting magnetic, electronic, optical, catalytic, thermal and mechanical properties. They are used in smart devices like intelligent machines (robots), personal computers, aircraft, automobiles, television, mobile telephones sensor etc, which have made our life comfortable and enjoyable. The requirement and challenge is in tailor-making these materials with desired composition, structure and properties. Materials Chemist have played an important role in this, due to their special talent, they are making use of these materials for various medical and other technological applications.

The Solid State Chemistry has become part of the formal training program in chemistry [1]. Being one of the frontiers of chemistry, it has a tremendous future and certainly demands the active involvement of many more chemists. The present time, Solid State Chemistry is mainly concerned with the development of new methods of synthesis, new ways of identifying, characterizing materials and describing their structure with desired and controllable properties.

Transition metal oxides constitute the most fascinating class of materials, exhibiting a variety of

\* Author for Correspondence: [y\\_havanoor@rediffmail.com](mailto:y_havanoor@rediffmail.com)

structures and properties [2]. The metal-oxygen bond can vary anywhere between highly ionic to covalent or metallic. The unusual properties of transition metal oxides are clearly due to the unique nature of the outer d-electrons. The phenomenal range of electronic and magnetic properties, exhibited by transition metal oxides is noteworthy. Thus, the electrical resistivity in oxide materials spans the wide range of  $10^{-10}$  to  $10^{20} \Omega \text{ cm}$ . We have oxides with metallic properties (e.g.  $\text{RuO}_2$ ,  $\text{RuO}_3$ ) at one end of the range and oxides with highly insulating behavior (e.g.  $\text{BaTiO}_3$ ) at the other. There are also oxides that transverse both, these regimes with changes in temperature, pressure or composition (e.g.  $\text{V}_2\text{O}_3$ ,  $\text{La}_{1-x}\text{Sr}_x\text{VO}_3$ ). Interesting electronic properties also arise from charge density wave (e.g.  $\text{K}_{0.3}\text{MoO}_3$ ), charge ordering (e.g.  $\text{Fe}_3\text{O}_4$ ) and defect ordering (e.g.  $\text{Ca}_2\text{Mn}_2\text{O}_5$ ,  $\text{Ca}_2\text{Fe}_2\text{O}_5$ ). Oxides with diverse magnetic properties anywhere from ferromagnetism (e.g.  $\text{CrO}_2$ ,  $\text{La}_{0.5}\text{Sr}_{0.5}\text{MnO}_3$ ) to antiferromagnetism (e.g.  $\text{NiO}$ ,  $\text{LaCrO}_3$ ,  $\alpha\text{-Fe}_2\text{O}_3$ ) are known. Many oxides possess switchable orientation states as in ferroelectric (e.g.  $\text{BaTiO}_3$ ,  $\text{KNbO}_3$ ) and ferroelastic [e.g.  $\text{Gd}_2(\text{MoO}_4)_3$ ] materials. Then, there are a variety of oxide bronzes showing a gamut of property [3]. Superconductivity in transition metal oxides has been known for some time and the highest  $T_c$  reached in the HTSC compounds (e.g.  $\text{YBa}_2\text{Cu}_3\text{O}_{7-y}$ ) was around 90 K; we now have oxides with  $T_c$  in the region of 160 K. The discovery of high  $T_c$  superconductors [4] has focused worldwide scientific attention on the chemistry of metal oxides and, at the same time, revealed the inadequacy of our understanding of these materials. The giant magneto resistance phenomenon in manganese oxides has attracted great attention [5].

The unusual properties of transition metal oxides that distinguish them from different phases are due to several factors:

- Oxides of d-block transition elements have narrow electronic bands, because of the small overlap between the metal d-orbital and the oxygen p-orbital. The bandwidths are typically of the order of 1-2 eV (rather than 5-15 eV as in most non metals).
- Electron correlation effects play an important role, as expected because of the narrow electronic bands. The local electronic structure can be described in terms of atomic like states [e.g.  $\text{Cu}^+(\text{d}^{10})$ ,  $\text{Cu}^{2+}(\text{d}^9)$  and  $\text{Cu}^{3+}(\text{d}^8)$  for Cu in  $\text{CuO}$ ] as in the Heitler-London limit.
- The polarizability of oxygen is also of importance. The divalent oxide ion  $\text{O}^{2-}$  does not exactly describe the state of oxygen and configurations such as  $\text{O}^-$  have to be included especially in the solid state which gives rise to polaronic and bipolaronic effects. Species, such as  $\text{O}^-$  which are oxygen holes with a  $\text{p}^5$  configuration instead of filled  $\text{p}^6$  configuration of  $\text{O}^{2-}$ , can be made mobile and correlated.
- Many transition metal oxides are not truly three-dimensional but also have low-dimensional features [6].

In the present investigation, we have made use of this novel synthetic route employing two immiscible liquids such as toluene and water, with the metal organic precursor (ferric acetylacetonate) in the organic layer and the hydrolyzing agent in the aqueous layer. Similarly, the synthesis of  $\text{CuO}$  metal oxide a suitable organic derivative metal taken in the organic layer reacts at the interface with the appropriate reagent present in the organic layer. Importance was given to the synthesis of  $\text{CuO}$  in this article.

Liquid-Liquid interface method is a one-step synthesis enabling synthesis of nanocrystal arrays at the liquid-liquid interface under ambient conditions. The diameters range of the nanoneedle form 2-8 nm and the lengths range from 30-100nm. These nanoneedles are distributed irregularly throughout the grid. Very fine particles of 8-10 nm are also besides the needles on careful observations. The TEM results suggest that the sample is light crystallinity in nature.

Most of above mentioned applications require the nanoparticles to be chemically stable and uniform in development of synthetic procedures to iron oxide nanoparticles, such as template methods [7, 8], micro-wave and  $\gamma$ -irradiation methods [9], sonolysis [10], microemulsion methods [11] thermal decomposition method [12,13], solvothermal method [14], Langmuir-Blodgett techniques [15], microwave technique [16] etc. Many of these methods involved in the synthesis of metal oxides are

tedious, some of them time consuming with many reaction steps and often suffer from the difficulty of tedious post-treatment procedures and reproducibility and also the formation of agglomerates cannot be ruled out. In contrast to the other methods, interfaces between immiscible liquids is a one step process enabling synthesis of nanocrystal arrays at the liquid-liquid interface and this method is known to be ideal for assembling of colloidal particles [17, 18]. Brust et al. [19] used immiscible water-organic solvent mixtures in the presence of phase-transferring reagents to prepare metal organosols. Rao et al. [20] have carried out an extensive experiment on nanocrystalline films obtained at the interface and found them to be essentially single crystalline in nature. Experiments by Rao et al., also revealed that it was indeed possible to prepare nanocrystals of metals [21-22] and other materials at the liquid-liquid interface through the reaction of an organometallic precursor taken in the organic layer with an appropriate reagent in the aqueous layer.

## **2. Materials and Methods:**

Ferrous ammonium sulphate hexahydrate, alcoholic solution of 8-hydroxy quinoline, dry acetone, Copper sulphate ( $\text{CuSO}_4$ ), acetylacetone, Sodium hydroxide (NaOH) and other chemicals used were AR grade. These solvents well purified and double distilled water were used.

### **2.1 Synthesis of $\text{Fe}_2\text{O}_3$ metal oxide using Liquid-Liquid Interfacial Method:**

Ultra fine films of inorganic materials have been prepared by a variety of methods. Physical methods such as thermal evaporation, laser ablation, vacuum sputtering and molecular beam epitaxy basically involved the evaporation of the reactants using high energy followed by condensation on a substrate yielding thin films of materials, Chemical methods such as chemical vapour deposition (CVD) and electro deposition generally employed in milder conditions. Thin films of nanocrystals have been prepared employing the Langmuir-Blodgett [LB] technique in the recent past and other materials have been prepared at the air water interface by the LB technique. The features and properties of a thin film generally depend on the nature of the substrate as well as on the technique and conditions employed for generating the film. Thus, thin films of inorganic materials are often polycrystalline or possess island structures. Since it is not always easy to obtain robust films of nanocrystals through self-assembly, it would be of great advantage to devise a suitable method of obtaining ultra thin films which are continuous over a wide area and are single crystalline in nature. In this context, the use of the liquid-liquid interface for generating nanocrystalline films of metals, metal-chalcogenides, and metal oxides is significant between immiscible liquids and are known to be ideal for assembling of colloidal particles.

Liquid-Liquid interface method is a one-step synthesis enabling synthesis of nanocrystal arrays at the liquid-liquid interface under ambient conditions. The method involves the reaction of an organometallic compound dissolved in the organic layer with reducing, sulfiding, or an oxidizing agent in the aqueous layer. The material formed at the interface is an ultra-thin nanocrystalline film, consisting of closely packed nanocrystals. A careful examination has shown that the materials formed at the interface is an ultra-thin nanocrystalline film consisting of closely packed metal/metal oxide nanocrystals coated with the organic species present at the interface. The other advantages of this invention are as follows: mild reaction conditions, easy to operate, short process period and easy to industrialize.

## **3. Characterization techniques:**

### **3.1 X-ray diffraction:**

Since the discovery in 1912 by Von Laue, X-ray diffraction has provided a wealth of important information to science and industry. For much that is to be known about the arrangement and the spacing of atoms in crystalline materials has been directly deduced from diffraction studies. These studies proved to be of immense importance in understanding the physical properties of metals, metal oxides and other solids non-destructively. The application of X-ray diffraction methods to chemical analysis is primarily in the identification of compounds present from their diffraction patterns and determination of the relative concentration by the intensities of pattern lines.

W.L. Bragg showed from the below equation that the X-rays reflected from a lattice plane and the effect associated with it could be derived by the equation.

$$n\lambda = 2d \sin\theta$$

Where 'n' is an integer (the "order"),  $\lambda$  the wavelength of the X-rays, d the inter-planar spacing and  $\theta$  is the angle of incidence of the X-ray beam on the lattice plane.

In crystalline powder, the tiny crystals are oriented at random. If an X-ray beam strikes such a powder, many planes will be so oriented, that Bragg's law is simultaneously satisfied and an X-ray diffraction pattern is obtained. To be certain that all possible planes are exposed to the X-ray beam, the specimen is usually rotated by an angle  $\theta$  on its own axis during exposure. Most of the X-ray beam will pass directly through the sample and diffracted beams, which are collected by a detector (scintillation counter). It is rotated by  $2\theta$  the output of which is processed and then fed into an automatic recorder. The result is a chart which gives a record of counts per second (proportional and diffracted beam intensity) versus diffraction angle  $2\theta$ .

The X-ray powder diffraction patterns of the solid sample or films were obtained using JEOL JDX-8P X-ray diffractometer. The target used was Cu  $K_\alpha$  or Co  $K_\alpha$  radiation. The X-ray generator was operated at 30 kV and 20 mA. The scanning range,  $2\theta/\theta$  was selected. The scanning speed =  $1^\circ$  or  $4^\circ \text{ min}^{-1}$ , chart speed =  $20 \text{ mm min}^{-1}$  were employed for precise lattice parameter determination. High purity silicon powder was used as an internal standard.

The d spacing of cubic ferrites, for a given set of planes (hkl) is given by:

$$d_{hkl} = \frac{n\lambda}{2 \sin \theta}$$

Where  $\lambda$  = wave length of the X-ray radiation in Å.

n = order of reflection and

$\theta$  = glancing angle of incidence.

### 3.2 Determination of average crystallite sizes from X-ray line broadening

The average crystallite size (D) from X-ray line broadening has been calculated using the Scherer equation (23-24)

$$D = \frac{0.9 \lambda}{\beta_{1/2} \cos \theta}$$

Where  $\lambda$  is the wavelength of the X-ray beam;  $\beta_{1/2}$  is the angular width at the half-maximum intensity and  $\theta$  is the Bragg angle. The instrumental broadening was collected using quartz as internal standard.

### 3.3 Density evaluation from X-ray data

The X-ray density of the sample have been computed from the values of lattice parameters for cubic system, using the formula [25]

$$d = \frac{8M}{Na^3}$$

Where 8 represents the number of molecules in a unit cell of a spinel lattice

M = Molecular weight of the ferrite sample

N = Avogadro's number, and

A = lattice parameter of the ferrite

The lattice constant a for cubic was calculated using equation

$$d = \frac{a}{(h^2 + k^2 + l^2)^{1/2}}$$

### 3.4 Infrared spectroscopy:

Infrared spectroscopy has widely been used for the identification of the functional groups in organic compounds because of the fact that their spectra are generally complex and provide numerous peaks that can be used for comparison purpose. In fact the infrared absorption spectrum of an organic compound is a fingerprint of its functional groups.

An infrared spectrum for metal oxides has been reported to some extent in literature. The main reason for this study includes Characterization of metal-oxygen frequencies and detecting the presence of

water along with impurities if any, identification of M-O peaks characterizes a particular class of compounds (e.g., two peaks one at 450 and other at 540  $\text{cm}^{-1}$  are the characteristic peaks for the spinel compounds).

It is also understood that the presence of water of hydration in the spinel ferrites give rise to stability of the ferrite, which is understood from the infrared studies.

From application and instrumentation point of view, the infrared region has been subdivided into three parts.

- near infrared region 4290-400  $\text{cm}^{-1}$  (0.7-2.5  $\mu\text{m}$ );
- middle infrared region 4000-666  $\text{cm}^{-1}$  (2.5-15  $\mu\text{m}$ ); and
- far-Infrared region 700-200  $\text{cm}^{-1}$  (14.3-50  $\mu\text{m}$ ).

In the present investigation, the infrared spectra of nano particles were recorded on a Perkin-Elmer FTIR spectrophotometer [Model 1000] in the range 400  $\text{cm}^{-1}$  to 4000  $\text{cm}^{-1}$ .

### 3.5 Scanning Electron Microscopy (SEM)

The shape, size and distribution of the grains of the powders, for the as prepared oxide samples, have been examined using a Leica-440 Cambridge Stereo scan, scanning electron microscope images. The SEM was operated at 20 kV. The samples were made conducting by the sputtering of gold using a 'Poloron DC sputtering unit' operated at 1.4 kV and 18-20 mA current. The SEM micrographs were taken using OR WO 35 mm film.

### 3.6 Transmission Electron Micrograph:

The shape, size, nucleation and growth of grains can be observed by the as prepared oxide samples, have been examined using Technai-20 Philips for high resolution of nanoscopic images. The powdered sample was suspended in deionized water and the suspended particles are sonicated for 30 minutes, after sonication a drop of suspension was taken on a copper grid with carbon supported film. The sample was allowed to dry and then inserted for transmission scanning. The TEM was operated at 190 keV.

### 3.7 Density Measurements:

#### Tap Density:

The as-prepared voluminous oxide materials were hand crushed in agate mortar using a pestle and a known amount of this powder was filled into a graduated cylinder of 25 ml capacity. The cylinder was tapped until the powder level remains unchanged. The volume occupied by the powder was noted. The ratio between the weight of the substance and the volume gave tap density.

### 3.8 Powder Density:

The powder densities were measured using Archimedes principle with a pycnometer and xylene as a liquid medium. The pycnometer of volume 25 ml was used. The following weights were taken and used in the density calculation.

$$\rho_{\text{sample}} = \frac{(W_2 - W_1)\rho_{\text{sol}}}{(W_4 - W_3) + (W_2 - W_1)}$$

Weight of the bottle	= $W_1$ g
Weight of the bottle + substance	= $W_2$ g
Weight of the bottle + substance + xylene	= $W_3$ g
Weight of the bottle + xylene	= $W_4$ g
Density of xylene	= $\rho_{\text{sol}}$
Density of sample	= $\rho_{\text{sample}}$

## 4. Result and Discussion

### 4.1 Fourier transform infrared spectroscopy (FT-IR) studies of $\gamma\text{-Fe}_2\text{O}_3$

The Figure 1.1 shows the metal oxygen peaks of Fe and O observed in the region of 450 and 550  $\text{cm}^{-1}$  and peaks observed in the regions 3450  $\text{cm}^{-1}$  is due to water of hydration.

#### 4.2 Scanning Electron Microscopy (SEM) studies of $\gamma\text{-Fe}_2\text{O}_3$ :

Figure 1.2 show the primary use of Scanning Electron Microscopy (SEM) is the study of the surface topography of solid samples. Figure shows sample under low and high resolution respectively. Under low resolution the image shows that the particles are interconnected with needle shape nanosized dimension forming agglomerates. Most of the particles are needle in shape. The size of these agglomerates shows the particles around 1-10  $\mu\text{m}$ . Under high resolution the distributions of the particles are irregular with flake shape.

#### 4.3 Transmission Electron Micrograph studies of $\gamma\text{-Fe}_2\text{O}_3$ :

Transmission electron micrograph was employed to confirm the crystalline nature, size and shape of the as synthesized  $\gamma\text{-Fe}_2\text{O}_3$  particles. Figure 4.5 (a) shows bright TEM images  $\gamma\text{-Fe}_2\text{O}_3$  nanocrystals. The TEM images of  $\gamma\text{-Fe}_2\text{O}_3$  shows the dense assembly of nano crystals with interconnected each other with having the needle shape with self-association. Probably it is due to magnetic attraction. The particles essentially appeared needle shape and reasonably monodispersed and uniform size have 16-18 nm in size. These uniformly sized crystals have better crystallinity and magnetic properties than the nono particle obtained by other conventional methods.

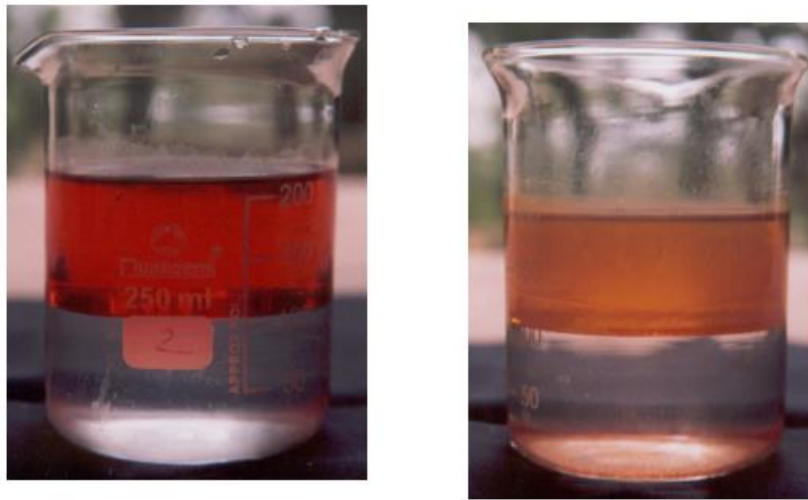
#### 4.4 Thermal Analysis of $\gamma\text{-Fe}_2\text{O}_3$ (TGA/DTA):

Figures 1.3 shows the TGA/ DTA traces of  $\text{J}_2$  (from ferric 8-hydroxy quinolate precursor), under a liquid nitrogen atmosphere. The general features observed from these traces are the dehydration step and the decomposition of organic moieties present in the  $\gamma\text{-Fe}_2\text{O}_3$ . The endothermic peak at 50  $^\circ\text{C}$  and its shoulder at 120  $^\circ\text{C}$  corresponds to loss of absorbed water molecules on the  $\gamma\text{-Fe}_2\text{O}_3$  sample, the second step is degradation which starts from 210  $^\circ\text{C}$  to 290  $^\circ\text{C}$  due to the decomposition of organic moieties present in the  $\gamma\text{-Fe}_2\text{O}_3$  sample. It is believed that the storage and liberation of energy with regard to deformation and annealing are important features in understanding the solid-state reactions. The recovery or recrystallisation, being the main energy releasing process of deformed solids, has been investigated exclusively on metals and metal carbonates [108]. At 390  $^\circ\text{C}$  the  $\gamma\text{-Fe}_2\text{O}_3$  has undergone phase transition to  $\alpha\text{-Fe}_2\text{O}_3$  i.e. a change from cubic to rhombohedral crystal system, which is indicated by the exothermic peak at 320 $^\circ\text{C}$  in its DTA curve.

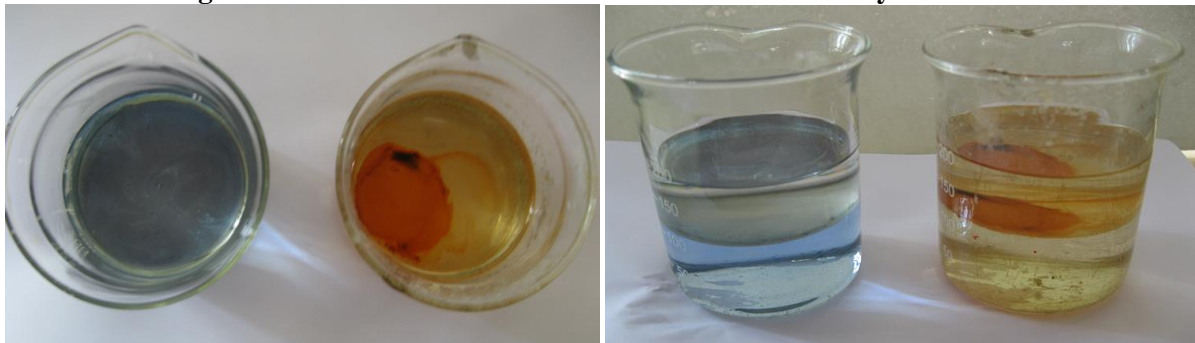
#### 4.5 Magnetic Iron oxide ( $\gamma\text{-Fe}_2\text{O}_3$ ):

Figure 1.4 shows the magnetic hysteresis loop for the magnetic nanocrystals measure at room temperature and  $T=85\text{ K}$ , in the range of  $H = \pm 10\text{ k Oe}$ . The figure shows that  $M_r$  and  $H_c$  231 and 18.75 Oe. The  $M_s$  value is 52.75 emu/g.





**Figure 1. shows interface reaction mixture of Ferric acetyl acetonate**



**Figure 2. shows interface reaction mixture of Copper acetyl acetonate**

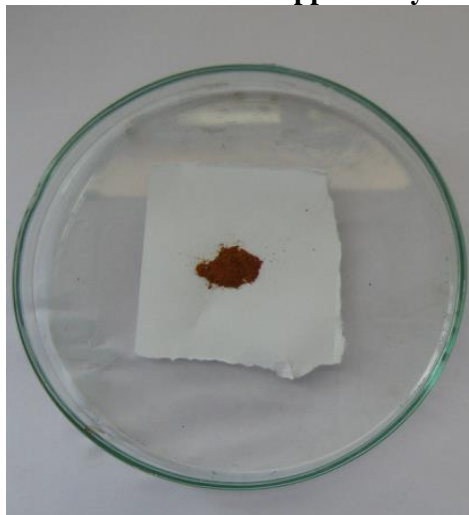


**Figure 3. shows the oxides of  $\gamma\text{-Fe}_2\text{O}_3$**

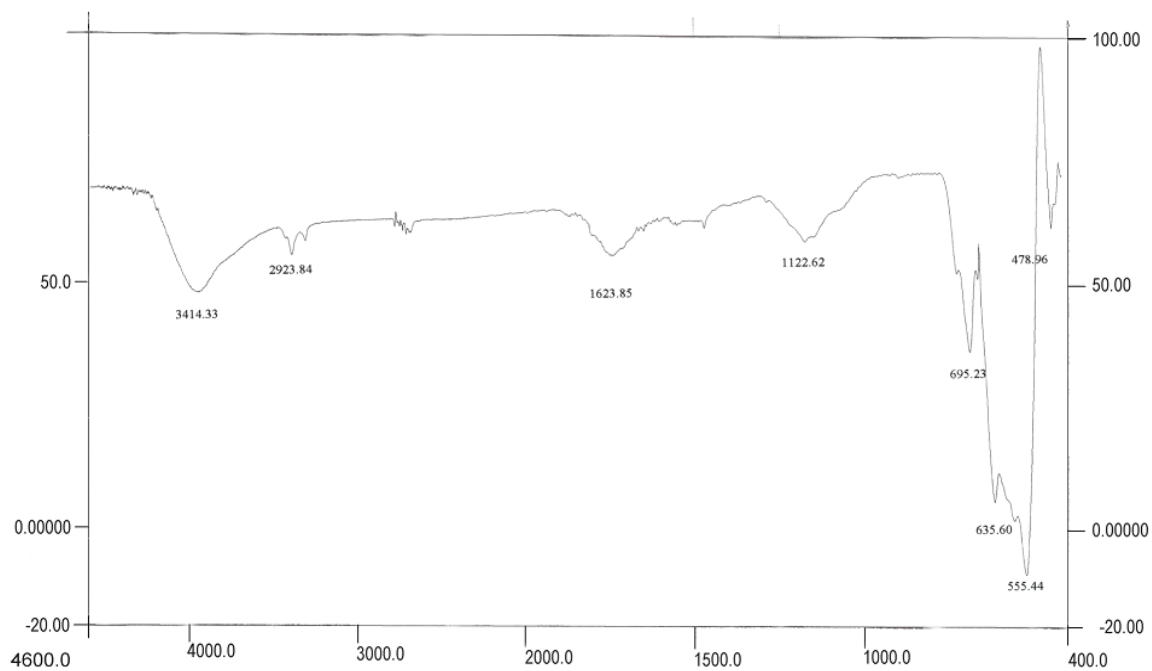


**Figure 4.** shows IR spectra of as synthesized  $\gamma$ -Fe<sub>2</sub>O<sub>3</sub> nanoparticles

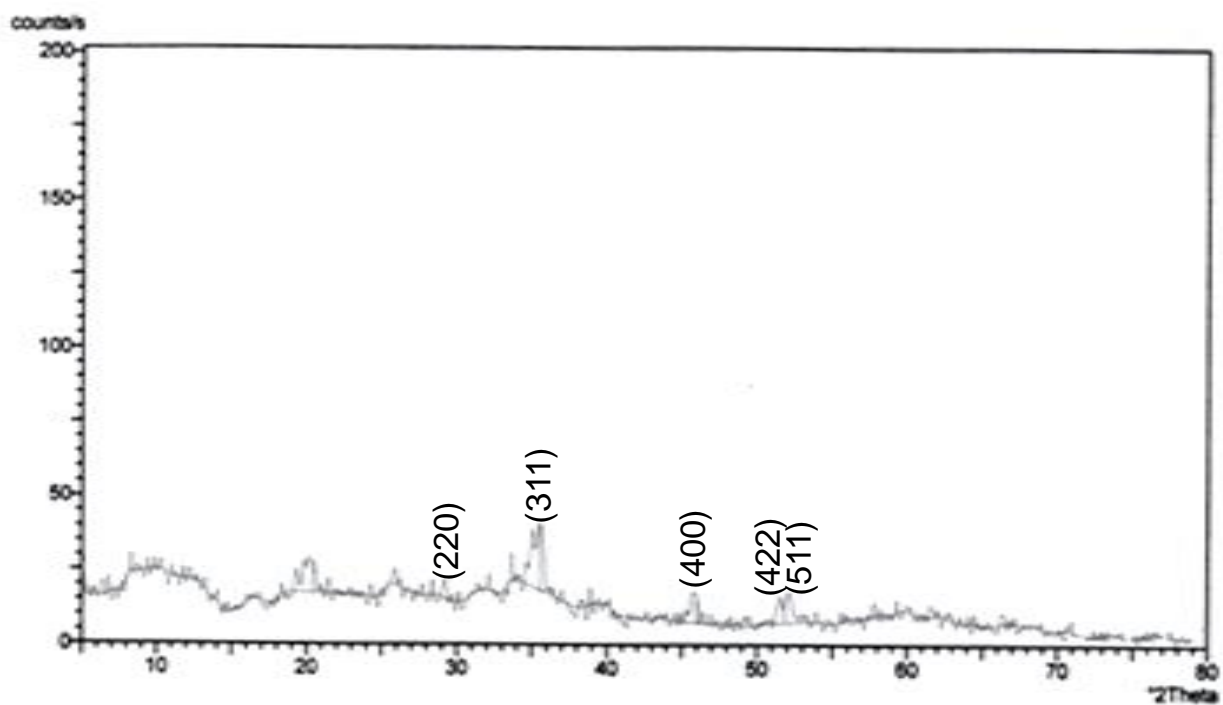


**Figure 5.** XRD pattern of as synthesized  $\gamma$ -Fe<sub>2</sub>O<sub>3</sub> nanoparticles.



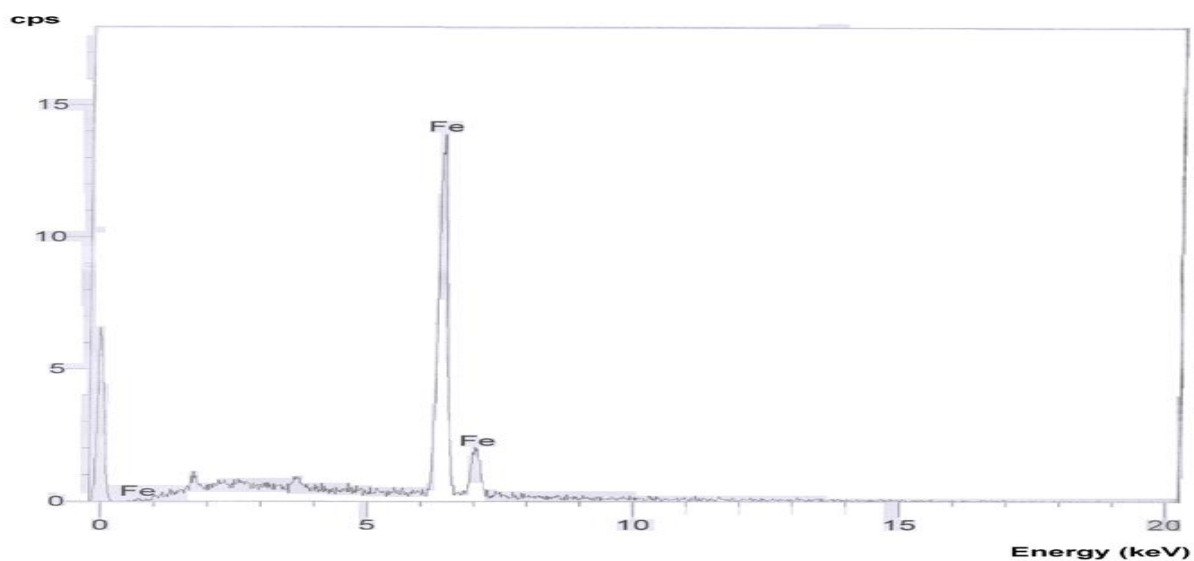
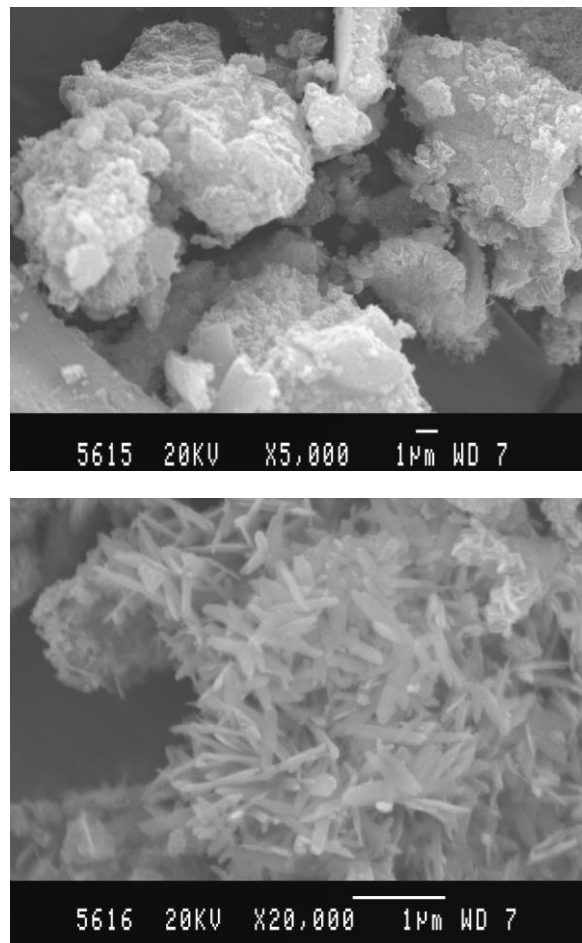


**Figure 6. EDAX pattern of as synthesized  $\gamma$ -Fe<sub>2</sub>O<sub>3</sub> nanoparticles**

**Table 1. Elemental analysis and densities of synthesized metal oxides  $\gamma$ -Fe<sub>2</sub>O<sub>3</sub>**

N%	ND	X-ray density (in Kg/m <sup>3</sup> )	3515
C%	5.56	Tap density (in Kg/m <sup>3</sup> )	4990
S%	ND	Bulk density (in Kg/m <sup>3</sup> )	5045
H%	2.77		



*SEM image of as synthesized  $\gamma\text{-Fe}_2\text{O}_3$*

**Figure 7. EDAX pattern of as synthesized  $\gamma\text{-Fe}_2\text{O}_3$  nanoparticles**



**Figure 8. TEM image of  $\gamma$ -Fe<sub>2</sub>O<sub>3</sub> nanoparticles.**

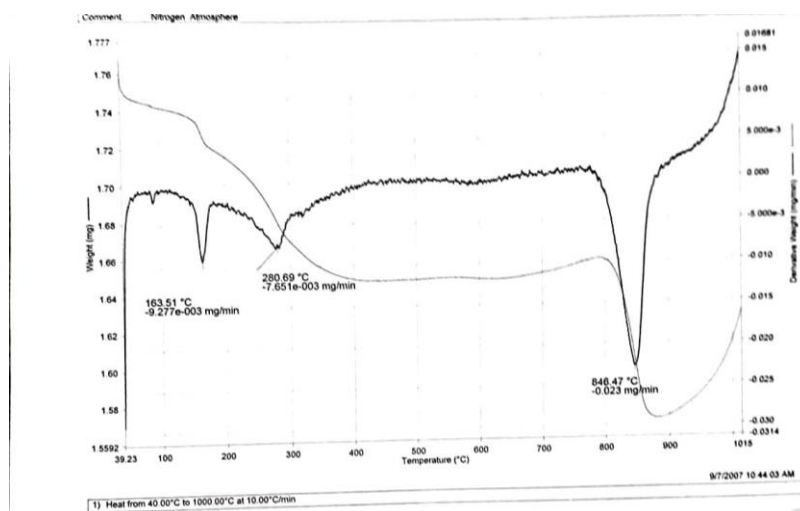


**Figure 9. Shows that Thermal analysis of  $\gamma$ -Fe<sub>2</sub>O<sub>3</sub> nanoparticles**

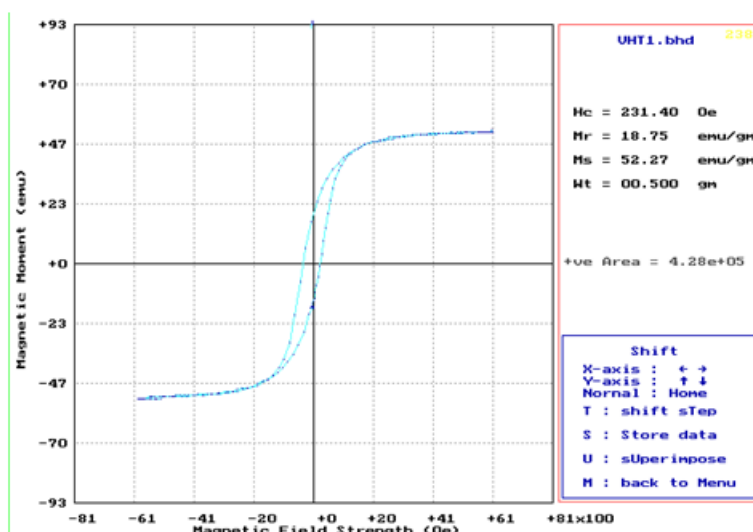


Figure 1.4. Shows that magnetic hysteresis loop of  $\gamma$ -Fe<sub>2</sub>O<sub>3</sub> nanoparticles

### Conclusion:

The experimental part includes the preparation of precursors of the respective metal complex which is dissolved in organic solvent and it is treated with alkaline medium (base), the reaction takes place at the interface and forms metal oxides consisting of nanosized particles. The characterizations of these metal oxides with IR, XRD, SEM and TEM give well authentic values with  $\gamma$ -Fe<sub>2</sub>O<sub>3</sub>. The method used for this is novel and advanced, low cost effective and high purity oxide are obtained.

### Reference:

1. C.N.R. Rao, Chemical approaches to the synthesis of inorganic materials, Wiley Eastern Ltd., New Delhi (1994)
2. J. Livage, M. Henry and C. Sanchez, Prog. Solid State Chem. 18 (1988)259.
3. R. Schollhorn, In inclusion compounds, J. L. Atwood, J. Davis and MacNicol, Ed., Academic press London 1. (1984) 249.
4. J. Rouxel, In, International layered Materials, F.Lavi (Ed). Reidel Publishing, Dordrecht, Holland (1979) 201.
5. L Babes, B. Denizot, G. Tanguy, J.J.L. Jeune and P. Jallet, J. Colloid Interf. Sci. 212 (1999) 474.
6. P. K Gupta and C.T Hung, Life Sci. 44 (1999) 175.
7. S. Liao, J. Zhu, W. Zhong, H. Y. Chen, Mater.Lett. 50 (2005)341.
8. A. Lagashetty V. Havanoor. S. Basawaraj, S. D. Balaji and A. Venkatraman, Sci. Technol. Adv. Mater. 8(2007)484.
9. J. Du and H. Liu, J. M. agen, Magen. Mater. 302 (2006)263.
10. J.Pinkas, V.Reichlova, R. Zboril, Z. Moravec, P.Bezdicka and J. Matejkova, Ultrason. Sonochem. 15 (2008) 257.
11. A. B. Chin and I. I. Yaacoob, J. Mater. Process Technol. 191 (2007) 235.
12. K. Woo, J. Hong, S. Choi, H-W. Lee, J-P.Ahn, C. S. Kim and S. W. Lee, Chem. Mater. 16 (2004) 2814.
13. T. Hyeon, S. S. Lee, J. Park, Y. Chung and H. B. Na, J.Amer. Chem. Soc.123 (2001) 12798.
14. S. Chaianansutcharit, O. Mekasuwandumrong and P. Praserttham, Cryst. Growth Des.6 (2006) 40.

*International Journal of Mechanical Engineering*

15. Q. Guo, X. Teng, S. Rahman and H. Yang, J. Amer. Chem. Soc. 125 (2003) 630.
16. Y. Lin, H. Skaff, T. Emrick, A. D Dinsmore and T. P Russsekkm Science 299 (2003) 226
17. M. Brust, M. Walker ,DBethell, D. J. Schiffrin and R. Whyman,. J. ChemSco. ChemCommuy, 7 (1994), 801
18. U. K Gautam . M. Ghosh and C,. N. R Rao, Langmuir 20(2004) 10775
19. C. N. R. RaoGu. U. Kkulkarni, P. J Thomas, V. V. Agrwal. And P. Sarvanan, J. Phys. Chem B 107 (2003)7391
20. C. N. R Rao G. U. Kulkarni P. J. Thomas V. V. Agrwal, U. K. Gautam and M. Ghosh. Curr.Sci 85 (2003)104
21. C. N. R Rao G. U. Kulkarni, V.V. Agrawal. U.K Gautam. M Ghosh and T Tumkurkar, J. Colloid Interf. Sci. 289 (2005) 305
22. U.K.Gautam, M. Ghosh and C.N.R. Rao Chem Phys. Lett. 381 (2003)1.
23. A.R. West, "Solid State Chemistry and its Application" John Weily New York (1989).
24. V.V.S.S Sai Sundar, Ph.D Thesis, Indian Institute of Science Bangalore1995.
25. C.N.R. Rao, Chemical Approches to the Synthesis of Inorganic Materials, Weily Eastern Ltd, New Delhi (1994).